DOE/PC/88912--T7

ROLES OF ADDITIVES AND SURFACE CONTROL IN SLURRY ATOMIZATION

DOE/PC/88912--T7

GRANT NO. DE-FG22-88PC88912

DE91 005461

Interim report

September 1988 to September 1990.

Submitted to

the Department of Energy

by

Shirley. C. Tsai
Professor and Principal Investigator
Department of Chemical Engineering
California State University
Long Beach, CA 90840
Tel. #(213)985-7534

Received by OSTI

DEC 21 1990.

Graduate Students:
Brian Viers, Khashayar Ghazimorad, and Dale Botts
Undergraduate Students:
Nuragung Widjaja and Jon Peters

DISCLAIMER

This report was prepared as an account of work sponsored by an agency of the United States Government. Neither the United States Government nor any agency thereof, nor any of their employees, makes any warranty, express or implied, or assumes any legal liability or responsibility for the accuracy, completeness, or usefulness of any information, apparatus, product, or process disclosed, or represents that its use would not infringe privately owned rights. Reference herein to any specific commercial product, process, or service by trade name, trademark, manufacturer, or otherwise does not necessarily constitute or imply its endorsement, recommendation, or favoring by the United States Government or any agency thereof. The views and opinions of authors expressed herein do not necessarily state or reflect those of the United States Government or any agency thereof.

MASTER

DISTRIBUTION OF THIS DOCUMENT IS UNLIMITED

NOV 28 1990

DISCLAIMER

This report was prepared as an account of work sponsored by the United States Government. Neither the United States nor any agency thereof, nor any of their employees, makes any warranty, express or implied, or assumes any legal liability or responsibility for the accuracy, completeness, or usefulness of any information, apparatus, product, or process disclosed, or represents that its use would not infringe privately owned rights. Reference herein to any specific commercial product, process or service by trade name, mark, manufacturer, or otherwise, does not necessarily constitute or imply its endorsement, recommendation, or favoring by the United States Government or any agency thereof. The views and opinions of authors expressed herein do not necessarily state or reflect those of the United States Government or any agency thereof.

TECHNICAL STATUS

This technical report is being transmitted in advance of DOE review, and no further dissemination or publication will be made of the report without prior approval of the DOE Project/Program Manager.

PATENT STATUS

US/DOE Patent Clearance is not required prior to the publication of this document.

ROLES OF ADDITIVES AND SURFACE CONTROL IN SLURRY ATOMIZATION

GRANT NO. DE-FG22-88PC88912

Shirley. C. Tsai
Professor and Principal Investigator
Department of Chemical Engineering
California State University
Long Beach, CA 90840

SUMMARY

This interim report focuses on the effects of interparticle forces on the rheology and airblast atomization of micronized coal water slurry (CWS). We found that the CWS flow behavior index is determined by the relative importance of the interparticle van der Waals attraction and the interparticle electrostatic repulsion. The former intensifies as the Hamaker constant increases and the interparticle distance reduces while the latter increases as the particle surface charge density increases. The interparticle attraction causes particle aggregation, which breaks down at high shear rates, and thus leads to slurry pseudoplastic behavior. In contrast, the interparticle repulsion prevents particle aggregation and thus leads to Newtonian behavior. Both macroscopically homogenous pseudoplastic and Newtonian slurries are prepared via the use of additives such as glycerol and anionic dispersant. Both are atomized at low atomizing air pressures (less than 270 kPa) using twin-fluid jet atomizers of various distributor designs. We found that the atomized drop sizes of micronized coal water slurries substantially decrease as the atomizing air pressure exceeds a threshold value. The atomized drop sizes, represented by the mass median diameter scaled to an atomizer characteristic length (MMD/L_c), can be described by a three-parameter nondimensional model in terms of slurry-to- air mass ratio ($\dot{M}_S/\dot{M}_A$), the Weber number (We), and the Ohnesorge number (Z):

$$MMD/L_c = (1 + \dot{M}_S/\dot{M}_A)\{x2\ We^{-x1} + x3\ Z^{x1}\}$$

where We equals the ratio of aerodynamic force to surface tension and Z represents the viscous effect. This model is based on the classical wave mechanism, momentum balance and energy considerations. The exponent and coefficients are determined by the best least square fit of the model to the experimental results using the iterative generalized inverse method. Excellent agreement with coefficients of correlation of 0.96-0.97 has been obtained between the model and the experimental data. While slurry pseudoplasticity and particle presence play a significant role in slurry atomization, the high shear slurry viscosity based on the free stream slurry velocity during atomization, represented by the Ohnesorge number, dictates the atomized drop sizes. Presence of coal particles also causes a looser drop size distribution curve as compared to pure viscous liquids. Nevertheless, the effects of coal volume fraction, coal particle surface charge, liquid composition and liquid viscosity on slurry atomization can be accounted for by their effects on slurry rheology.

INTRODUCTION

Micronized coal water slurry has the potential to replace oil in utility and industrial boilers with little burner retrofitting because the residual ash in the deeply cleaned micronized coal can be transported out of boilers in the gas stream. Twin-fluid atomizers[1-4], when used in slurry combustion, have a number of advantages over pressure atomizers including lower slurry pressure, finer spray, and, thus, higher combustion efficiency. The twin-fluid jet atomizer used in this study is designed to minimize errosion of the nozzle tip. As shown in Fig. 1, the slurry passes axially through the center of the distributor. The atomizing air passes through the 15°-angled slits drilled in the 45° taper of the distributor and, thus, swirls around the slurry jet. The nozzle has a single discharge port of diameter larger than the diameter of the distributor for slurry passage. Atomizing air pressures as low as 150 kPa are used in order to examine the drop size (primary drop) resulting from ligament breakup. Low atomizing air pressures are also economically more desirable.

Presented in this interim report are: (1) the effects of interparticle forces on slurry rheology and how they affect slurry atomization, (2) nondimensional models for CWS atomization based on wave mechanism, momentum balance and energy considerations, and (3) Comparisons of micronized CWS atomization with airblast atomizations of viscous Newtonian and pseudoplastic liquids.

MATERIALS AND MEASUREMENTS

Micronized Upper Freeport coal and Illinois #6 coal are used in this study. The Upper Freeport coal is high volatile bituminous A, and has been cleaned by microbubble flotation to an ash content of 5.4% on dry basis. Other coal analyses are: 82.8% carbon, 5.1% hydrogen, 0.7% nitrogen, 1.2% sulfur, and 4.8% oxygen. The particle sizes of the Upper Freeport coal are batch #1: 3-5μ m with both volume mean and mass median diameters of 4.4 μm; and batch #2: 98% $<20\,\mu$m with volume mean and mass median diameters of 5 μm and 4 μm, respectively. The Illinois #6 coal is high volatile bituminous C, and has also been cleaned by microbubble flotation. Its analyses are: 75.2% carbon, 5.2% hydrogen, 2.5% sulfur, 1.4% nitrogen, 4.2% ash and 11.5% oxygen on dry basis. The particle sizes of Illinois #6 coal are 3-25 μm with 60% within 3 μm to 4 μm, volume mean diameter of 7.8 μm and mass median diameter of 3.7 μm. The lower-ranking Illinois #6 coal is more readily oxidized than the Upper Freeport coal[5]. Both are irregularly shaped and have a density of 1.33-1.37 g/cc. The liquids for slurry preparation include aqueous solutions of 20-80% glycerol or 42% ethylene glycol or 50% isopropanol, a 80/20 w/w mixture of ethylene glycol and glycerol, and water containing a small amount of an anionic dispersant (Coal Master A23M from Henckel Corporation containing 44 wt% naphthalene sulfonic acid formaldehyde polymer, ammonium salt). The water is deionized and other liquids are reagent grade. Irregularly shaped sand particles with 2.60 g/cc density, sieved to 20-40 μm by Alpine Air-Jet Siever, are also used for comparison of slurry rheology.

Atomization of micronized coal water slurries is carried out using one nozzle tip of 0.249 cm in diameter and three distributors whose dimensions are given in Table I. The nozzle tip is positioned 0.254 cm downstream from the distributor tip. Distributors #1 and #2 have a central opening 0.152 cm in diameter for slurry flow and

have no internal chamber. Distributor #3, used in slurry combustion[6], has a central opening 0.244 cm in diameter for slurry flow and an internal chamber 0.40 cm in diameter and 0.16 cm in length where the slurry meets the atomizing air prior to discharging to atmosphere. Slurry flow rates vary from 1.0 to 4.7 g/s depending upon the atomizing air and slurry pressures. Distributor #1 is used in the atomization of slurries a), d), e), and f); distributor #2 in slurries c), d), and f); and distributor #3 in slurries b) and e). The properties of these slurries are given in Table II.

While the drop size and size distribution are measured using the Malvern Particle Sizer 2600C, the slurry viscosity is measured using the Brookfield rotational viscometer RVTD at shear rates $<20\ s^{-1}$, and the Burrell-Severs capillary rheometer A120 at shear rates $>20\ s^{-1}$. The liquid viscosities are also measured by the Haake rotational viscometer RV20. The zeta potential is measured using the Malvern Zeta Sizer IIc, and the surface tension of the suspending liquids is measured using the Fisher Scientific Surface Tensiometer Model 20. Detailed descriptions of the experimental methods, atomization setup, and data analysis are given in the papers published by this PI's group[7-10].

SLURRY RHEOLOGY

The slurry rheology is characterized by the Ostwald-de Waele power law of $\tau = K\dot{\gamma}^n$, where τ, $\dot{\gamma}$, n, and K are the shear stress, shear rate, flow behavior index, and flow consistency index, respectively.

Correlation between the Slurry Flow Behavior Index and the Hamaker Constant

We have found that the flow behavior index of a concentrated suspension is determined by the relative importance of the interparticle van der Waals attraction and the interparticle electrostatic repulsion[11]. The interparticle attraction, measured by the Hamaker constant scaled to the thermal energy at ambient temperature (A/kT), causes particle aggregation, which breaks down at high shear rates, and thus leads to pseudoplastic behavior ($n < 1$). In contrast, the interparticle repulsion prevents particle aggregation and thus leads to the Newtonian behavior of well dispersed systems. It should be noted that the zeta potential in deionized water is a qualitative measure of the particle surface charge density and, thus, is indicative of the relative interparticle electrostatic repulsion[12].

At constant particle volume fraction and surface charge density (measured by the zeta potential in deionized water), n decreases linearly as A/kT increases as shown in Fig. 2. Also shown in Fig. 2 are results on concentrated suspensions of polystyrene spheres (circles), glass beads (diamond), and silica (diamond) sand[9-11,13,14] for comparison. Table III lists the Hamaker constants (A/kT) of coal particles, polystyrene spheres, and glass beads suspended in various liquids as calculated by the Lifshitz equation[15]:

$$A/kT = 3/4\ \{(\varepsilon_1 - \varepsilon_3)/(\varepsilon_1 + \varepsilon_3)\}^2 + 3\ h\ \nu_e(n_1^2 - n_3^2)^2 / \{16\ 2^{1/2}(n_1^2 + n_3^2)^{3/2}\} \quad (1)$$

where h and k are the Planck and Boltzman constants, respectively; ε_1 and ε_3 are, respectively, the dielectric constants of particle and the suspending liquid; n_1 and n_3 are the corresponding refractive indices; ν_e is the absorption frequency. The

Hamaker constant of coal suspended in a liquid mixture is assumed to be the sum of those of coal in pure liquids multiplied by the liquid volume fractions. Also given in this table are the liquid viscosities. The dielectric constant[16], the refractive index[17], and the absorption frequency[16] of coal are 2.89, 1.701, and $1.15 \times 10^{16}\ s^{-1}$, respectively. The dielectric constants and the refractive indices of the liquids and the other solids as well as the liquid viscosities are supplied by the manufacturer (General Electric for silicone oils) or taken from the CRC Handbook of Chemistry and Physics.

Table IV lists our experimental results on the slurry flow behavior indices and the corresponding shear rate ranges within which these indices are measured. Our earlier results on concentrated suspensions of polstyrene spheres, glass beads and sand are also listed for discussion. In our earlier study, we found that suspensions of glass beads (average diameters of 31 μm and 45 μm) in silicone oils (viscosities of 0.52 P, 1.1 P, and 9.5 P) at volume fractions of 0.55, 0.58, and 0.60 are Newtonian ($n = 1$)[10] in agreement with the negligible Hamaker constant. Recently, we found that suspensions of irregularly shaped silica sand in silicone oils at particle volume fractions of 0.50, 0.52, and 0.55 are also Newtonian[11]. This Newtonian behavior of glass beads and silica sands in silicone oils, represented by the diamond at A/kT of 0.2 in Fig. 2 was verified by repeatition and by varying the particle volume fraction and the liquid viscosity. In addition, our earlier study[10] on concentrated suspensions of polystyrene (average diameters of 6 μm and 78 μm) in ethylene glycol (viscosity of 0.17 P) shows that particle size has no significant effect on the flow behavior index of the concentrated suspension (within 3%). The average flow behavior index of the polystyrene suspensions at 0.55 volume fraction is shown in Fig. 2 (open circle at A/kT of 1.1). Likewise, 0.55 volume fraction suspensions of glass beads of different sizes with average diameters of 23 μm, 31 μm, and 45 μm in ethylene glycol and glycerol give rise to similar flow behavior indices (within 5%). The average value is also shown in this figure (diamond at A/kT of 0.6). Based on these results, we conclude that neither the size and shape of particles with aspect ratio close to unity nor the viscosity of liquids is capable of making the Newtonian suspensions behave like pseudoplastic materials. In contrast, a good correlation between the flow behavior index and the Hamaker constant can be seen in Fig. 2 for such diverse suspensions. In this regard, it should be mentioned that the zeta potential of the polystyrene spheres (6 μm) in deionized water is found to be very small (-4.5 mV). Therefore, we believe that the interparticular electrostatic repulsion is negligible in the nonaqueous polystyrene suspensions, and the interparticle van der Waals attraction is the predominating force that affects their flow behavior.

Fig. 2 also shows that the flow behavior index of a glycerol/water suspension of Upper Freeport Coal (volume mean diameter of 4.4 μm and zeta potential of 24 mV in deionized water) at 0.47 particle volume fraction (open triangles) varies linearly with the Hamaker constant A/kT. The four triangles at A/kT ranging from 3.0 to 3.3 in this figure represent the Upper Freeport coal slurries in aqueous solutions of a variety of alcohols with various viscosities as listed in Table III. It should be noted that the flow behavior index of the polystyrene spheres (45 μm) in silicone oil suspension at 0.45 particle volume fraction[14] (solid circle in Fig. 2) also falls on this line.

The flow behavior indices of suspensions containing 0.40 volume fraction of slightly oxidized Upper Freeport coal (volume mean diameter of 4.4 μm and zeta potential of -2 mV in deionized water) and surface oxidized Illinois #6 coal (volume mean diameter of 3.7 μm and zeta potential of -30 mV in deionized water) in aqueous solutions of 80% and 40% glycerol are also shown in Fig. 2. (inverted triangles and squares, respectively). The more negative zeta potential of the lower-ranking and more severely oxidized Illinois #6 coal relative to the Upper Freeport coal[5] is expected to give rise to a greater interparticular electrostatic repulsion in aqueous suspensions of the same coal volume fraction. The Illinois #6 coal slurries are therefore more Newtonian than the Upper Freeport coal slurries at 0.40 volume fraction as shown in Fig. 2. This figure also shows that while the interparticular electrostatic repulsion has a significant effect on the flow behavior of these coal water slurries, the correlation between n and A/kT still holds at both 0.40 and 0.47 volume fractions. Moreover, the suspension becomes less pseudoplastic (n increases) as the volume fraction decreases. This result is in good agreement with what has been reported on polystyrene in silicone oil suspensions[14], and can be attributed to increased interparticle distance. In fact, Fig. 2 shows that the increased interparticular van der Waals attraction due to a decreased interparticle distance in the 0.47 volume fraction suspension with respect to the 0.40 volume fraction suspension outbalances the increased interparticular electrostatic repulsion due to its higher zeta potential. The Upper Freeport coal slurry is more pseudoplastic at 0.47 volume fraction than at 0.40 volume fraction as a result. It should be noted that the polystyrene (45 μm) in silicone oil suspension at 0.40 volume fraction is Newtonian[14], Its flow behavior index is in line with the aqueous suspensions of the mildly oxidized Upper Freeport coal (4.4 μm and zeta potential of -2 mv in deionized water) at the same volume fraction (see Fig. 2).

In order to further verify the role of interparticle electrostatic repulsion force in slurry rheology, an anionic dispersant (Coal Master A23M from Henckel Corporation) is adsorbed onto the surface of Upper Freeport coal particles to increase its surface charge density. We found that as the anionic polymer concentration increases from 0.36% to 0.74% by weight of coal, the zeta potential of the coal in deionized water decreases from +4 to -35 mV. As a result, the flow behavior index of the Upper Freeport CWS at 0.48 volume fraction increases from 0.83 to 1.0. Likewise, as shown in Fig. 3, the pseudoplastic Upper Freeport CWS at 0.46 volume fraction becomes nearly Newtonian (n equals 0.94) as the anionic polymer concentration increases from 0.32 % to 0.49 % by weight of coal.

Relative Slurry Viscosity as a Function of Particle Peclet Number

The relative slurry viscosity is defined as the ratio of the slurry viscosity to the viscosity of the suspending liquid. The particle Peclet number, or called reduced shear rate[18], equals the time required for a particle to diffuse a distance comparable to its radius multiplied by the shear rate. Fig. 3 shows that the relative viscosities of the Upper Freeport coal in water/glycerol (28/72 w/w with liquid viscosity of 0.28 P) slurry are in line with those of the sand in ethylene glycol/glycerol (80/20 wt/wt with liquid viscosity of 0.35 P) slurry, both at 0.45 volume fraction (solid circles and solid diamonds, respectively). It should be noted that both coal and sand particles are irregularly shaped but their densities differ substantially (1.33 vs 2.60 g/cc). Also shown in this figure for comparison are our earlier results[10] on the relative vis-

cosities of 0.55 volume fraction suspensions of polystyrene spheres (open circles, narrowly sized with volume mean diameters of 6 μm and 75 μm with a density of 1.05 g/cc) and glass beads (open inverted triangles and open triangles for unsieved and sieved to 20-40 μm glass beads #5000 from Potter Industry, respectively) in ethylene glycol (0.17 P) and 80/20 w/w ethylene glycol/glycerol mixture (0.35 P). Based on these results, we conclude that the relative slurry viscosity is independent of particle density.

Fig. 3 also shows that the relative viscosities of the Upper Freeport coal slurry containing an aqueous solution of 50 wt% isopropanol at 0.46 volume fraction (open squares) are considerably higher than those of the Upper Freeport coal in 28/72 w/w water/glycerol slurry at 0.45 volume fraction (solid circles). The substantial increase in the relative viscosity, much more than what can be accounted for by the increase in the volume fraction from 0.45 to 0.46, can be attributed to the nearly one order of magnitude decrease in the viscosity of the suspending liquid (0.28 P vs 0.04 P). Note that the zeta potential in deionized water for this Upper Freeport coal is +4 mV, and therefore the primary force affecting the rheology of these water/alcohol or glycerol slurries is the interparticle van der Waals attraction. The relative viscosities of the Upper Freeport CWS at 0.46 volume fraction containing 0.32 wt% anionic polymer (open diamonds) are only slightly lower than those of the Upper Freeport coal slurries containing aqueous solutions of 50 wt% isopropanol (liquid viscosity of 0.04 P) at the same volume fraction (open squares). In contrast, increasing the concentration of the anionic dispersant not only renders the slurry Newtonian as mentioned earlier but also considerably enhances the relative viscosity (see Table V) as compared with the rigid sphere model[19] using the maximum packing fraction of 0.50 obtained from sedimentation of Newtonian suspensions of narrowly sized (20-40 μm), irregularly shaped sand as the scaling factor:

$$\eta_r = (1 - \phi/0.50)^{-1.34} \qquad (2)$$

The underlying mechanisms are under investigation.

Based on the above rheology study, coal water slurries of various flow behavior indices and viscosities can be prepared by varying the coal volume fraction, the coal surface charge density, and the compositions of the suspensing liquids. Six coal water slurries thus prepared are atomized. As shown in Table II, these coal water slurries are composed of 0.40-0.47 volume fraction of micronized Upper Freeport coal and Illinois #6 coal in aqueous solutions of 20-40% glycerol or 42% ethylene glycerol or in water containing anionic dispersant at a concentration of 0.49% of polymer by weight of coal. Slurries a) through d) are pseudoplastic with flow behavior indices ranging from 0.50 to 0.58 because the interparticular van der Waals attraction predominates over the interparticular electrostatic repulsion. As shown in Table II, slurry e) is less pseudoplastic with a flow behavior index of 0.82 because of its smaller volume fraction and greater interparticle electrostatic repulsion. Slurry f), in which the hydrophobic coal particles are dispersed in water by anionic polymer, is nearly Newtonian with a flow behavior index of 0.94. The nearly constant viscosity of slurry f) serves as a reference to determine the viscosity effect on CWS atomization of unknown flow field.

As shown in Fig. 4, slurries c) and d) are considerably less viscous than slurries a) and b) throughout the entire shear rate range from 20 to 7000 s^{-1}. This figure also shows that the viscosity of slurry f) varies from 6.5 P at 400 s^{-1} to 4.5 P at 3000 s^{-1}. The latter equals the respective viscosities of slurry c) at 2000 s^{-1} and slurry b) at 4500 s^{-1}. The viscosity of slurry e), which is more viscous than slurry f), varies from 17 P at 200 s^{-1} to 10 P at 2000 s^{-1}. It is less viscous than slurries c) and d) at shear rates less than 200 s^{-1}, but more viscous than slurries a) and b) at shear rates above 2000 s^{-1}. Within the shear rate range of 400 to 2000 s^{-1}, slurry e) is more viscous than slurries c) and d), but less viscous than slurries a) and b). While slurries a) and b) have similar viscosities (40-12 P) at shear rates between 50 and 1000 s^{-1}, their viscosities at high shear rates (2000 s^{-1}) are significantly different (less than 9 P and 8 P for slurry a) and slurry b), respectively). In contrast, the viscosities of slurries c) and d) at shear rates above 400 s^{-1} are similar.

SLURRY ATOMIZATION

As the atomizing air swirls downstream arround the jet, waves form on the jet surface. The amplitudes of these waves grow exponentially if their wavelengths exceed a minimum value based on classical wave mechanism[20,21]. As a result, the jet sheds ligaments which subsequently collapse into small drops. Both regressional analysis of drop MMDs and examination of drop size distributions indicate that the effects of slurry rheology, including the effects of coal fraction and liquid composition, on slurry atomization can be accounted for in terms of three nondimensional groups, namely, the slurry- to-air mass ratio ($\dot{M}_S/\dot{M}_A$), the Weber number (We), and the Ohnesorge number (Z). The wave mechanism-based models[4] established for primary atomization of viscous Newtonian liquids are found to fit the slurry atomization data with coefficients of correlation of 0.96-0.97 (see Fig. 5). Like in glycerol atomization[4], a threshold atomizing air pressure exists in the airblast atomization of micronized coal water slurries. When the inlet atomizing air pressures exceed this threshold value, the MMD/$(1 + \dot{M}_S/\dot{M}_A)$ is considerably smaller. This phenomenon may be attributed to the sudden expansion at the nozzle tip when the atomizing air reaches the maximum velocity (sonic velocity)[4,22]. This threshold pressure varies from 170 to 240 kPa depending on the distributor design[8]. Furthermore, the coefficient of correlation deteriorates to 0.77 if all of the experimental data are grouped together with no consideration of this threshold pressure. Detailed discussion of these models and effects now follows.

Wave Mechanism-based Models

Atomization is a process whereby a volume of liquid is converted into waves, ligaments, and ultimately into a multiplicity of small drops[20,21]. The waves are initiated by such factors as pressure fluctuation or turbulence in the gas stream or the liquid stream[21]. They continue as capillary waves if surface tension predominates, and as acceleration waves if aerodynamic pressure force dominates. The dynamic pressure ($\rho_A V_A^2/2$) of the air stream in airblast atomization is large enough that the amplitude of the surface waves will grow if their wavelength (λ) exceeds a minimum value[20]. When the amplitude becomes sufficiently large, the waves generate ligaments that are shed and rapidly collapse, forming drops. The amplitude (A) of the surface waves on the liquid jet is described by the following differential equation[20]:

$$dA/dt = A\{[\pi \beta \rho_A (V_A-u)^2] / (\lambda \rho_S u) - (8 \pi^2 \eta_S) / (\lambda^2 \rho_S)\} \quad (1)$$

In this equation, we see that the amplitude, damped by the liquid viscous force, increases as the relative air velocity increases. When both the aerodynamic pressure and the surface tension forces are important, the wave velocity u is given[20] by

$$u = [(a \lambda / 2 \pi) + (2 \pi \sigma_L / \lambda \rho_S)]^{1/2} \quad (2)$$

where σ_L is the surface tension of the liquid, and the acceleration a is caused by the aerodynamic drag on the liquid jet in terms of free stream aerodynamic pressure. Since $V_A > u$ Eqs. (1) and (2) show that the amplitude growth is resisted by the surface tension.

The minimum wavelength λ_m, above which the amplitude grows exponentially with time, may be estimated by setting $dA/dt = 0$. This results in the following cubic expression for λ_m:

$$\lambda_m^3 - \lambda_a \lambda_m^2 - \lambda_\sigma^3 = 0 \quad (3)$$

where $\lambda_\sigma/D = \{2\pi(16)^{1/3}/\beta^{2/3}\} (Z/We)^{2/3}$ (3a)

$\lambda_a/D = \{64 C_{Do} \sin^2\theta / N\beta^2 \pi\} (Z^2/We)$ (3b)

the Weber number (We) equals $\rho_A V_A^2 D/\sigma_L$, representing the ratio of aerodynamic force to surface tension, the Ohnesorge number (Z) equals $\eta_S/(\rho_S \sigma_L D)^{1/2}$, and the shock dynamic pressure ratio (N) equals $\rho_A V_A^2/\bar{\rho}_A \bar{V}_A^2$ with respect to the free stream aerodynamic pressure.

When the aerodynamic pressure force predominates, waves propagate as acceleration waves at a minimum velocity of $(a \lambda_m/2\pi)^{1/2}$. In this case, $\lambda_a << \lambda_\sigma$, and one solution to Eq. (3) is $\lambda_m = \lambda_\sigma$ which is governed by $(Z/We)^{2/3}$ as shown in Eq. (3a). In contrast, when the surface tension predominates, waves propagate as capillary waves at a minimum velocity of $(2\pi \sigma_L / \lambda_m \rho_S)^{1/2}$. Since $\lambda_\sigma << \lambda_a$, one solution to Eq. (3) is $\lambda_m = \lambda_a$, which is governed by (Z^2/We) as shown in Eq. (3b). Therefore, both We and Z, with the exponent of Z- dependency equal to or twice that of We^{-1}-dependency, are included in our modeling of drop sizes. These semi-empirical models are:

$$MMD/L_c = (1 + \dot{M}_S/\dot{M}_A)\{x2\ We^{-x1} + x3\ Z^{x1}\} \quad (4a)$$
$$MMD/L_c = (1 + \dot{M}_S/\dot{M}_A)\{x2\ We^{-x1} + x3\ Z^{2\ x1}\} \quad (4b)$$
$$MMD/L_c = (1 + \dot{M}_S/\dot{M}_A)\{x2(Z/We)^{x1} + x3\} \quad (4c)$$
$$MMD/L_c = (1 + \dot{M}_S/\dot{M}_A)\{x2(Z^2/We)^{x1} + x3\} \quad (4d)$$

where the linear scale factor L_c is equal to 0.152 cm, one of the distributor diameters for slurry passage, D in We and Z denotes the diameter of the distributor in use for slurry flow during atomization. Therefore, the Weber number at the same ratio of aerodynamic pressure to surface tension is greater in distributor #3 than in dis-

tributor #1 because of its larger diameter for slurry flow. The reverse is true for the Ohnesorge number. It should be noted that the effect of atomizer size on slurry atomization is accounted for by D in both We and Z while L_c is simply a scale factor to render MMD nondimensional.

A linear dependency on $1 + \dot{M}_S/\dot{M}_A$ is used in this study based on the momentum balance[23]:

$$\dot{M}_S V_S + \dot{M}_A V_A = (\dot{M}_S + \dot{M}_A)V \qquad (5)$$

where V is the velocity of the atomized drop and the atomizing air after transferring part of its kinetic energy to the slurry. We assume that the total surface energy of the atomized drops is proportional to the loss of kinetic energy:

$$\Sigma \dot{N}_i D_i^{\,2} \sigma_S \;\alpha\; \{(\dot{M}_S V_S^{\,2} + \dot{M}_A V_A^{\,2}) - (\dot{M}_S + \dot{M}_A)V^2 \qquad (6)$$

where $\dot{N}_i$ is the number of drops with a diameter D_i produced per unit time, and σ_S is the drop surface energy per unit area. Substituting Eq. (5) and $\dot{M}_S = \rho_S \Sigma \dot{N}_i D_i^{\,3}$ $\pi/8$ into Expression (6) yields

$$\text{SMD} \;\alpha\; (1 + \dot{M}_S/\dot{M}_A)$$

where the Sauter mean diameter (SMD) equals $\Sigma \dot{N}_i D_i^{\,3} / \Sigma \dot{N}_i D_i^{\,2}$. It should be noted that $(1 + \dot{M}_L/\dot{M}_A)$ was used in the basic equation for prefilming atomizer[24] although exponents ranging from 0.4 to 2 were reported for airblast atomization of low viscosity liquids[25].

Since the flow field in airblast atomization is unknown, which viscosity should be used in the calculation of the Ohnesorge number for atomization of pseudoplastic CWS must be determined first. Fig. 6 shows that although the drop MMDs of all slurries obtained at atomizing air inlet pressures above the threshold value under comparable atomization conditions are quite similar, the MMDs of slurry e) atomized at inlet air pressures below the threshold value are significantly larger than those of slurry a) atomized under comparable conditions. It should be noted that the viscosity of slurry e) at shear rates above 2000 s^{-1} is greater than that of slurry a), but smaller at shear rates below 2000 s^{-1}. Likewise, Table VI shows that slurry e) is much more difficult to atomize at atomization air pressure below the threshold value (similar drop MMDs are obtained at lower slurry- to-mass ratio and larger Weber number) than slurry d) because slurry e) is much more viscous at shear rates above 1000 s^{-1} even though they have similar viscosities at shear rates between 100-300 s^{-1} (see Fig. 4). Fig. 6 also shows that the MMDs of the nearly Newtonian slurry f) with viscosities ranging from 6.5 P to 4.5 P in a shear rate range of 400 to 3000 s^{-1} are in line with those of the pseudoplastic slurries a), b), and d) whose high shear viscosities range from 4 P to 6.5 P depending on the prevailing shear rate conditions during atomization. Therefore, the high shear slurry viscosity based on the free

stream slurry velocity at atomization conditions, equivalent to shear rates above 2000 s^{-1} and sometimes as high as 10,000 s^{-1}, is chosen in calculation of Z. The effects of slurry rheology will be further discussed later.

Iterative computation using the generalized inverse method[26] is carried out to determine the exponents and the coefficients of Eqs. (4a) through (4d) by the best least squares fit of these equations to 44 experimental data points. Wide ranges of the aforementioned nondimensional groups are covered:

$1+\dot{M}_S/\dot{M}_A$	We	Z
1.65-6.70	65-1065	0.60-3.25

Eqs. (4c) and (4d) consistently give poorer coefficients of correlation (as low as 0.91 for atomization at inlet air pressure above the threshold value) than Eqs. (4a) and (4b). Therefore, only Eqs. (4a) and (4b) with the best least squares solutions obtained from the iterative generalized inverse method are listed in Table VII. Fig. 5 demonstrates the excellent agreement between the experimental data and the 3-parameter models (Eqs. (4a) and (4b)) with the listed best least squares solutions. The coefficients of correlation for atomizations at air pressures below and above the threshold value are 0.97 and 0.95-0.96, respectively. The slightly poorer agreement for atomization at air pressures above the threshold value may be attributed to the high percentage of the smaller than 20 μm drops, and indicate that these small drops may result from breakup of the primary drops rather than ligament shedding (see Figs. 7 and 8). It should be noted that the coefficient of correlation in Table VII is reduced by at least 1% when any one of these parameters exceeds the given range. Regressional analysis using the exponent of $(1+\dot{M}_S/\dot{M}_A)$ as an additional parameter does not improve the coefficient of correlation and yields a solution close to unity.

Effect of Distributor Design

As shown in Fig. 9, the atomization air mass flow rate using distributor #1 varies with the absolute inlet air pressure similarly for slurries a) and e). These atomizing air mass flow rates at constant inlet pressures are higher than those for atomization of slurry d), but substantially lower than those for atomization of glycerol using the same distributor and nozzle. Also shown in this figure is saturation of atomizing air mass flow rate at high inlet pressures in the glycerol atomization using distributor #1[4]. Such a saturation phenomenon is also seen in the atomization of slurry d) using a distributor of smaller cross section (distributor #2) for air flow, and may also be attributed to the achievement of maximum air velocity (sonic velocity) at the atomizer tip[22].

Fig. 9 also shows that the mass flow rate of the atomizing air varies with the distributor design. Distributor #1 gives rise to the highest air mass flow rate at a constant inlet air pressure as a result of its largest cross section for air flow and much smaller diameter for slurry flow relative to the discharge port (0.152 cm vs 0.249 cm). Distributor #3 gives rise to the smallest air mass flow rate because its diameter for slurry flow is only slightly smaller than that of the discharge port (0.244 cm vs 0.249 cm). At the same inlet air pressure, distributor #2 gives rise to a smaller air

mass flow rate than distributor #1 due to its smaller cross section. However, it gives rise to a much higher velocity and, thus, a much higher Weber number as shown in Table VIII.

Also shown in Table VIII, the distributor design has a substantial effect on $(1 + \dot{M}_S/\dot{M}_A)$. At same absolute inlet pressures of atomizing air and slurry (190 kPa and 253 kPa, respectively), distributor #3 gives rise to the largest $(1 + \dot{M}_S/\dot{M}_A)$ while maitains a high Weber number. Distributor #1 gives rise to the smallest $(1 + \dot{M}_S/\dot{M}_A)$. The aforementioned threshold air pressures effecting better atomization for both distributors are less than 190 kPa. Distributor #2 which gives rise to the largest Weber number yields intermediate $(1 + \dot{M}_S/\dot{M}_A)$. However, the threshold air pressure for this distributor appears to be higher than 190 kPa. As a result, use of distributor #2 in the atomization of slurry d) gives rise to considerably larger drop MMD (125 μm vs 74 μm) and MMD/$(1 + \dot{M}_S/\dot{M}_A)$ (42 vs 30) than distributor #1.

Nevertheless, regressional analyses for atomization below and above the threshold air pressure show that drop MMD in both cases varies with the slurry-to-air mass ratio, the Weber number, and the Ohnesorge number in similar manners for all distributors. Furthermore, the atomized drop size distributions with similar MMDs are independent of distributor design. For example, as shown in Fig. 8, the drop size distribution of atomized slurry d) with 340 μm MMD from distributor #1 is similar to that with 338 μm MMD from distributor #2, and the drop size distribution with 51 μm MMD from distributor #2 lies between those with 74 μm MMD and 45 μm MMD from distributor #1 (see Table VI for the atomization conditions).

Effects of Coal Volume Fraction and Liquid Composition

As shown in Fig. 4, although the flow behavior index increases only slightly, the slurry viscosity decreases considerably as the coal volume fraction decreases from 0.47 in slurry a) to 0.43 in slurry c). From Table VI, we see that the drop MMD obtained from atomization of slurry c) at atomizing air pressure below the threshold value is significantly smaller than that from slurry a). This result can be attributed to a higher We due to the use of distributor #2 and a smaller Z due to a much lower viscosity of slurry c).

A slightly looser drop size distribution is seen in Fig. 7 for atomized slurry c) with respect to slurry a). This appears to be true for slurry f) with a 0.46 volume fraction (see Fig. 8) but with a high shear viscosity (3-4 P) close to that of slurry c). Therefore, we believe that the looser drop size distribution is attributable to the lower slurry viscosity rather than the difference in coal fraction. Similar looser drop size distribution is seen in atomized 92/8 w/w glycerol/water mixture with 3.8 P viscosity as compared with glycerol with 9.8 P viscosity. (see Fig. 9)

Because of its much lower viscosity, slurry d) can be atomized to similar MMDs at less severe atomization conditions than slurry a) (see Table VI). Nevertheless, a comparison between Figs. 7 and 8 shows that the drop size distributions of atomized slurry d) (42% ethylene glycol suspension at 0.43 coal volume fraction) are very similar to those of atomized slurry a) (40% glycerol suspension at 0.47 coal volume

fraction) at comparable MMDs. Therefore, we conclude that the slurry rheology, rather than the coal fraction or the liquid composition, dictates the drop size and size distribution in airblast atomization of micronized coal water slurries.

Effects of Slurry Rheology

As mentioned earlier, the effects of slurry rheology on slurry atomization drop sizes can be described in terms of the Ohnesorge number based on the high shear slurry viscosity. Table VI shows that the effect of slurry rheology on the drop MMD is more pronounced for atomization at air pressures below the threshold value than above the threshold pressure. Within the ranges used, both We and Z terms make contributions of same order of magnitude to the drop MMD for atomization at inlet pressures below the threshold value. The We-term dominates for atomizing air pressures above the threshold value. This is further illustrated in Fig. 6 in which the lines (slope of unity) represent the MMD dependency on $1 + \dot{M}_S/\dot{M}_A$. When atomized at inlet air pressures below the threshold value, slurry e) gives rise to much larger MMDs than slurries a) and d) because of its much larger high shear viscosity (7-8 P for slurry e), 4 P for slurry a), and 2-3 P for slurry d)). In contrast, when atomized at inlet air pressures above the threshold value all slurries generate similar drop MMDs at comparable Weber numbers. Note that the high shear viscosities at these atomization conditions for slurries e), a), b), and f) are 7-8 P, 6-7 P, 5-7 P, and 4-5 P, respectively, while those for slurries c) and d) are 2-3 P.

Comparison with Viscous Liquid Atomization

Also given in Fig. 6 for comparison are the drop MMDs of atomized glycerol (9.8 P, open circles and open triangles) and its aqueous solution containing 92% glycerol (3.8 P, open inverse triangles), and atomized pseudoplastic polyethylene glycol (PEG) mixture (3.5/96.5 w/w) of molecular weights of 8000 and 600 with a flow behavior index of 0.78 and a high shear viscosity of 4 P (open diamonds). Open circles and open triangles in this figure designate glycerol atomized at Weber numbers ranging from 265 to 280, and from 415 to 460, respectively. The Weber numbers for PEG atomization (open diamonds) range from 240 to 305. The numbers next to the clusters of solid points in the figure are the Weber numbers for CWS atomization. From this figure we see that slurry f) which is nearly Newtonian with 4.5 P high shear viscosity atomizes to similar drop sizes at comparable atomization conditions as the pseudoplastic PEG mixture. Slurry f) requires a higher air velocity (greater Weber number) than glycerol to atomize to similar MMDs. Fig. 6 also shows that at atomization air pressures below the threshold pressure, it is more difficult to atomize pseudoplastic slurry e) with high shear viscosities of 7 to 8 P than to atomize glycerol. The reverse is true for atomization air pressures above the threshold value. The atomization behaviors of pseudoplastic slurry a) with high shear viscosities of 4-7 P and pseudoplastic slurry d) with high shear viscosities of 2-3 P are similar to that of glycerol (9.8 P). Both atomize less readily than aqueous glycerol with a viscosity of 3.8 P. Thus, although the high shear viscosity dictates the atomized drop sizes, the slurry pseudoplasticity and the presence of coal particles appear to have detrimental effects on atomization.

A comparison between the drop size distributions of the atomized slurries (Fig. 7 for slurry a) and Fig. 8 for slurries d) and f)) and the atomized glycerol and its aqueous solution (Fig. 10) reveals that drop sizes with peak intensity at 350 μm appear in the slurry atomization as well as in the atomization of glycerol and its aqueous solution. Neither the chemical composition of the liquid mixture (glycerol vs ethylene glycol vs water) nor the presence of coal particles has any significant effect on these primary drop sizes. In contrast, considerable differences in the distributions of smaller sizes are seen between the atomized slurries and the atomized glycerol. A very high percentage of drop sizes smaller than 20 μm is produced when either glycerol or aqueous glycerol is atomized at inlet air pressures above the threshold value. Except for slurry f) at atomizing air pressures above the threshold value, the percentage of smaller than 20 μm drops is negligible in the atomized slurries. Both slurries and aqueous glycerol solutions yield high percentages of 40-50 μm drops. In fact, except for the smaller than 20 μm sizes, the slurry drop size distribution curve is quite similar to that of the 3.8 P aqueous solution containing 92% glycerol; both have a looser structure with respect to the atomized glycerol (9.8 P). This looser structure of drop size distribution curve may be attributed to disruption of the continuous phase by impurities such as water and coal particles.

A comparison between the atomized slurry drops (Figs. 7 and 8) and the atomized PEG drops (Fig. 10) also reveals similar drop sizes and size distributions at atomization conditions which result in drop MMDs of 70 μm and larger. At severe atomization conditions which result in MMD of 50 μm and smaller, a much tighter size distribution curve and a significant percentage of smaller than 20 μm drops are seen for the pseudoplastic PEG mixture.

CONCLUSIONS

This study clearly demonstrates that the CWS flow behavior index is determined by the relative importance of the interparticle van der Waals attraction and the interparticle electrostatic repulsion. The interparticle attraction causes particle aggregation, which breaks down at high shear rates, and thus leads to pseudoplastic behavior. In contrast, the interparticle repulsion prevents particle aggregation and thus leads to Newtonian behavior. While the slurry pseudoplasticity and the presence of coal particles play a signicant role in airblast atomization of micronized CWS, the high shear slurry viscosity dictates the atomized drop size and size distribution. Coal volume fraction and liquid composition affect slurry atomization via their effects on slurry rheology. The wave mechanism-based semi-empirical model is shown to describe drop MMDs of atomized micronized CWS in terms of three nondimensional groups, $1 + \dot{M}_S/\dot{M}_A$, We, and Z. The overall drop size distributions of the atomized slurries resemble those of the atomized aqueous glycerol with 3.8 P viscosity and the atomized pseudoplastic polyethylene glycol mixture with n equaling 0.78 and a high shear viscosity of 4.5 P, and are quite different from those of glycerol with 9.8 P viscosity.

ACKNOWLEDGMENTS

This principal investigator gratefully acknowledge Drs. David Wildman and George Wen at the Pittsburgh Energy Technology Center for selection and supply of coals. Helpful discussions with Dr. Wildman is also greatly appreciated.

NOMENCLATURE

a	Acceleration
A	Hamaker constant or Amplitude of the surface waves on the liquid jet
C_{Do}	Drag coefficient
D	Diameter of liquid jet or atomizer distributor diameter
D_i	Diameter of atomized drop
L_c	Characteristic length
MMD	Mass median diameter of drops
$\dot{M}$	Mass flow rate
$\dot{N}$	Shock dynamic pressure ratio
N_i	Number of drops with diameter D_i produced per unit time
n, K	Flow behavior index and flow consistency index, respectively
P	Pressure or Poise
u	Wave velocity
V	Velocity or average velocity
VMD	Volume mean diameter
SMD	Sauter mean diameter
We	Weber number $\rho_A V_A^2 D/\sigma_L$
Z	Ohnesorge number, $\eta_S/(\rho_S \sigma_L D)^{1/2}$
ρ	Density
η	Viscosity
λ	Wavelength
β	Jeffreys' sheltering parameter having a value between 0 and 1.
θ	Angle between the jet axis and the free stream gas velocity
σ	Surface tension or surface energy per nit area
$\tau, \dot{\gamma}$	Shear stress and shear rate, respectively

Subscripts

A	Atomizing Air
L	Liquid
S	Slurry or particle

REFERENCES

1. For example, Manfred, R.K., Borio, E.W., Smith, D.A., Rini, M.J., LaFlash, R.C., and Marion, J.L., "Current Progress in Coal-Water Slurry Burner Development," *ACS Preprint, Division of Fuel Chemistry*, 28, 36-61, 1983.
2. Meyer, P.L. and Chigier, N., "The Atomization Process in Coal-Water Slurry Sprays," *Proc. of the 8th Int. Sym. on coal Slurry Fuels Preparation and Utilization*, 144-161, 1986.
3. Tsai, S. C. and Vu, T., "Atomization of Coal Water Slurry Using Twin-fluid Jet Atomizer," *Fuel*, 66, 1596-1602, 1987.
4. Tsai, S.C. and Viers, B., "Airblast Atomization of Viscous Liquids," to appear in *Fuel*, 1990.

5. Tsai, S.C., *Fundamentals of Coal Beneficiation and Utilization,* Coal Science and Technology Series, Vol. II, Elsevier Scientific Publishing Co., Ltd., Amsterdam/Oxford/London/New York, 1982.

6a. Knell, W. and Mansour, M.N., *Proceedings of the 5th International Symposium on Coal Slurry Combustion Technology*, 25-27 April 1983, Tempa, FL.

6b. Tsai, S. C. and Knell, E., "Rheology and Its Effects on Atomization of Coal Water Slurry," *Proc. of the First Annual Pittsburgh Coal Conference*, 190-200, 1984.

7. Tsai, S. C., Viers, B. and Botts, D., "Effects of Pseudoplastic Behavior on Airblast Atomization of Viscous Liquids," *Proceedings of the ASME 3rd International Symposium on Liquid-Solid Flows,* FED-75, 225-231, 1988.

8. Tsai S. C., Ghazimorad, K., and Viers, B., "Airblast Atomization of Micronized Coal slurries Using Twin-fluid Jet Atomizer," to appear in *Fuel.*

9. Tsai S. C. and Viers, B., "Effect of Liquid Polarity on Rheology of Noncolloidal Suspensions," *J. of Rheology*, 31, 483-494, 1987.

10. Tsai, S. C. and Zammouri, K., "Role of Interparticular Van der Waals Force in Rheology of Concentrated Suspensions," *J. of Rheology*, 32, 737-750, 1988.

11. Tsai S. C. and Ghazimorad, K., "Correlation between the Flow Behavior Index of a concentrated Suspension and the Hamaker Constant," to appear in *J. of Rheology*, 1990.

12. Loeb, A.L., Overbeek, J.Th.G., and P.H. Wiersema, *The Electrical Double Layer Around a SphericalColloid Particle*, the M.I.T. Press, Massachusetts Institute of Technology, Cambridge, Mas sachusetts, 1961.

13. Tsai, S.C., Botts, D., and B. Viers, "Effects of Liquid Viscosity on Rheology of Concentrated Suspensions," *Particulate Science and Technology*, 7, 87-95, 1989.

14. Gadala-Maria, F., and A. Acrivos, "Shear Induced Structure in a Concentrated Suspension of Solid Spheres," *J. of Rheology*, 24, 799- 814, 1980.

15. Israelachvili, J.N., *Intermolecular and Surface Forces*, Chapter 11, 137-160, Academic Press, New York/San Francisco/London, 1985.

16. Reynolds, W.N., *Physical Properties of Graphite*, Elsevier Publishing Co., Ltd., Amsterdam/ London/New York, 1968.

17. Mellor, J.W., A *Comprehensive Treatise on Inorganic and Theoretical Chemistry*, Vol V, p.767. Longmans, 1724.

18. Russel, W.B., "Review of the Role of Colloidal Forces in the Rheology of Suspensions," *J. of Rheology*, 24, 287-317, 1980.

19. Krieger, I.M., "Rheology of Monodisperse Latices," *Advance Colloid Interface Science*, 3, *111*-136, 1972.

20. Jeffreys, H., "On the Formation of Water Waves by Wind", *Roy. Soc. Proc.*, A107, 189-206, 1925.

21. Adelberg, M., "Mean Drop Size Resulting from the Injection of a Liquid Jet into a High-Speed Gas Stream," *AIAA*, 6, 1143-1147, 1968.

22. Kihm, K.D. and Chigier, N., "The Influence of Sonic Air Flows on Liquid Atomization of Airblast Atomizers", Extended Abstracts, 131-135, *The 3rd Annual Conference of Institute of Liquid Atomization and Spray Systems*, Irvine, CA, 1989.

23. Wigg, L. D., "Drop-size Prediction for Twin-fluid Atomizers," *J. of Institute of Fuel*, 27, 500-505, 1964.

24. Lefebvre, A. H., "Airblast Atomization," *Progr. Energy Combustion Science*, 6, 233-261, 1980.

25. For a summary of drop size equations reported in the literature, see Tables 6.9 through 6.11, Chapter 6, Lefebvre, A. H., *Atomization and Sprays,* Hemisphere Publishing Corp., New York/London, 1989.

26. Fletcher, R., "Generalized Inverse Methods for the Best Least Squares Solution of Systems of non-linear Equations", *Computer J.*, 10, 392-399, 1968.

TABLE I
ATOMIZER DIMENSIONS

Nozzle tip No.	Discharge Diameter cm	Cross Section cm^2
1	0.249	4.866×10^{-2}

Distributor No.	Slit Design dia. cm*	No.-cm x cm	Cross Section, cm^2 Liquid	Air
1	0.152	4-0.24 x 0.076	1.815×10^{-2}	7.354×10^{-2}
2	0.152	6-0.076x 0.086	1.815×10^{-2}	3.950×10^{-2}
3#	0.244	6-0.086x 0.114	4.676×10^{-2}	5.925×10^{-2}

*Diameter of the central opening for slurry flow
#Variflo atomizer by Delavan Corp., South Carlorina

TABLE II
PROPERTIES OF COAL SLURRIES AND SUSPENDING LIQUIDS

Slurry	Flow** Behav. ind. n	Consist indx K	Coal Vol. Fraction	Suspending liquid Conc. wt%	Visco. cP	S. Tension* dyne/cm
a)	0.54	290	0.47 UpF1	40% glcerl	3.6	71
b)	0.50	308	0.47 UpF1	20% glcerl	1.7	72.2
c)	0.58	145	0.43 UpF1	40% glcerl	3.6	71
d)	0.52	175	0.43 UpF2	42% glycol	3.0	65.5
e)	0.82	35	0.40 Ill #6	40% glcerl	3.6	71
f)	0.94	8.4	0.46 UpF2	water/disp#	1.	61

**Viscosity in P equals $K\dot{\gamma}^{n-1}$, where $\dot{\gamma}$ designates shear rate
*Surface tension is measured using the Fisher Surface Tensiometer Model 20, and the results are comparable with those obtained from the CRC Handbook of Chemistry and Physics.
#Dispersant (A23M) concentration of 0.49 % anionic polymer by wt. of coal

TABLE III
DIMENSIONLESS HAMAKER CONSTANT A/kT FOR INTERPARTICLE VAN DER WAALS ATTRACTION ACROSS VARIOUS SUSPENDING LIQUIDS

Solid/liquid	Polystyrene	Glass	Coal	Liq. viscosity, P
Silicone oil	1.1	0.2	2.0	0.52-9.5
Ethylene glycol	1.3	0.6	2.1	0.17
Glycerol	0.9	0.6	1.7	9.8
Water	--	1.2	3.7	0.01
80/20 w/w glycerol/water			2.2	0.60
40/60 w/w glycerol/water			3.0	0.036
20/80 w/w glycerol/water			3.3	0.017
50/50 w/w isopropanol/water			3.1	0.036
42/58 w/w ethylene glycol/water			3.1	0.030

TABLE IV

MEASURED FLOW BEHAVIOR INDEX OF A CONCENTRATED SUSPENSION AND THE CORRESPONDING SHEAR RATE RANGE

Solid	Vol. frac.	Liquid	n	Shear rate, s^{-1}	Reference
Glass beads	0.55-0.60	silicone oils	1.0	15-2000	Tsai, 1987
	0.55	glycerol	0.83	9-200	Tsai, 1989
Silica sand	0.50-0.55	silicone oils	1.0	20-700	Tsai, 1990
Polystyrene	0.55	silicone oils	0.76	2-400	Tsai, 1987
78 μm	0.58		0.78	0.5-350	
	0.55	ethyl. glycol	0.81	45-800	
	0.58		0.82	150-1500	
Polystyrene	0.55	ethyl. glycol	0.87	2-2500	Tsai, 1988
6 μm	0.58		0.85	1-1500	
	0.55	glycerol	0.85	10-200	
Polystyrene	0.55	silicone oils	0.86	0.04-50	Gadala-Maria
45 μm	0.45		0.96	0.15-50	& Acrivos,
	0.40		1.0	0.5-50	1980
Upper Freeport	0.47	80% glycerol	0.76	60-1000	Tsai, 1990
coal, 4.4 μm	0.47	40% glycerol	0.54	50-6000	
	0.47	20% glycerol	0.50	25-6000	
	0.47	50% i-propanol	0.58	20-500	
	0.45	42% glycol	0.58	30-1500	
	0.40	80% glycerol	0.82	40-1000	
	0.40	40% glycerol	0.67	200-2000	
Illinois #6	0.40	80% glycerol	0.93	20-500	Tsai, 1990
coal, 3.7 μm	0.40	40% glycerol	0.77	200-2000	

TABLE V

COMPARISON OF THE RELATIVE VISCOSITIES OF NEWTONIAN SLURRIES

Solid	Vol. frac.	Dispersant# coal basis	η_r, Expt.	η_r, Model 0.50 ϕ_M
Up. Fr. coal	0.48	anionic polym. 0.74 wt%	1150	75
Up. Fr. coal	0.45	anionic polym. 1.15 wt%	450	22
Sand, 20-40 μm	0.45	Silicone oil	22	22

#Dispersant is used in coal water slurries only, and water is replaced by silicone oil in the case of sand suspesnion.

TABLE VI EFFECTS OF DISTRIBUTOR DESIGN AND SLURRY RHEOLOGY ON SLURRY ATOMIZATION

Slurry	Distr No.	$1+\dot{M}_S/\dot{M}_A$	We	Z	P_A kPa	P_S kPa	MMD μm	$\frac{MMD}{1+\dot{M}_S/\dot{M}_A}$
d)	1	5.24	67	0.73	149	245	340	65
	2	6.70	285	0.60	156	280	338	50
	1	2.49	252	0.83	190	254	74	30
	2	2.77	1060	0.69	238	280	51	18
	1	2.26	288	0.85	212	254	45	20
	1	2.12	410	0.80	236	280	36	17
c)	2	4.97	749	0.76	183	252	224	45
	2	3.80	978	0.79	245	276	132	35
	2	3.26	1065	0.83	266	276	73	22
	2	3.30	1015	0.85	245	252	65	20
a)	1	4.42	204	1.98	183	333	271	61
	1	3.10	269	2.26	190	324	128	41
	1	2.05	252	3.08	170	249	74	36
	1	1.79	305	3.21	204	245	50	28
	1	1.76	447	2.91	244	280	36	20
e)	1	3.93	159	2.00	156	276	336	86
	1	2.88	217	2.09	167	252	246	85
	1	2.91	265	2.03	183	276	118	41
	1	2.39	265	2.14	190	252	62	26
	1	1.93	442	2.16	235	276	34	18
f)	1	5.03	148	1.41	149	256	324	64
	1	2.92	375	1.41	218	280	152	52
	1	2.99	204	1.44	204	252	132	44
	1	2.81	324	1.43	204	252	90	32
	1	2.43	324	1.44	225	258	44	18
	1	1.94	305	1.48	252	256	33	17
9.8 P glycerl		3.20	173	2.81	156	249	159	50
		2.81	502	2.81	204	314	74	26
		1.84	527	2.81	225	245	36	20
3.8 P glycerl-water		3.64	189	1.10	163	221	109	30
		4.43	224	1.10	218	266	54	12
		2.83	288	1.10	238	266	41	14
Polyethylene glycols		3.20	240	0.93	173	232	194	61
		3.12	272	0.91	197	266	175	56
		3.06	240	0.94	183	232	100	33
		2.34	325	0.97	228	242	50	21

TABLE VII

SEMI-EMPIRICAL MODEL FOR AIRBLAST ATOMIZATION OF MICRONIZED COAL WATER SLURRIES#

$$MMD/L_c = (1 + \dot{M}_S/\dot{M}_A)\{x2\ We^{-x1} + x3\ Z^{x1}\}\ 10^{-2} \quad (4a)$$

$$MMD/L_c = (1 + \dot{M}_S/\dot{M}_A)\{x2\ We^{-x1} + x3\ Z^{2\,x1}\}\ 10^{-2} \quad (4b)$$

	xl	x2	x3	c.o.c.*	Equation
(a)	0.22 ± 0.03	9.9 ± 1.0	0.49 ± 0.05	0.97	(4a)
(b)	0.32 ± 0.03	10.4 ± 1.0	0.21 ± 0.05	0.96	(4a)
(a)	0.22 ± 0.03	9.9 ± 1.0	0.48 ± 0.05	0.97	(4b)
(b)	0.33 ± 0.03	11.7 ± 1.0	0.16 ± 0.05	0.95	(4b)

L_c equals 0.152 cm

* Coefficient of correlation

(a) Atomizing air pressure below the threshold value

(b) Atomizing air pressure above the threshold value, MMD is replaced by volume mean diameter in the case of glycerol atomization

TABLE VIII

EFFECTS OF DISTRIBUTOR DESIGN ON SLURRY ATOMIZATION

Slurry	Distr No.	$1 + \dot{M}_S/\dot{M}_A$	We	Z	P_A kPa	P_S kPa	MMD μm	$\frac{MMD}{1 + \dot{M}S/\dot{M}A}$
d)	2	2.86	547	0.83	197	252	139	49
	2	2.98	647	0.78	190	252	125	42
	1	2.49	252	0.83	190	254	74	30
	2	2.77	1060	0.69	238	280	51	18
	1	2.12	410	0.80	236	280	36	17
e)	1	2.39	265	2.14	190	252	62	26
	1	1.93	442	2.16	235	276	34	18
	3	5.00	426	1.88	190	254	141	28
	3	3.99	519	1.91	225	254	87	22
	3	3.40	655	1.93	252	254	57	17

Fig. 1 Design of twin-fluid atomizer

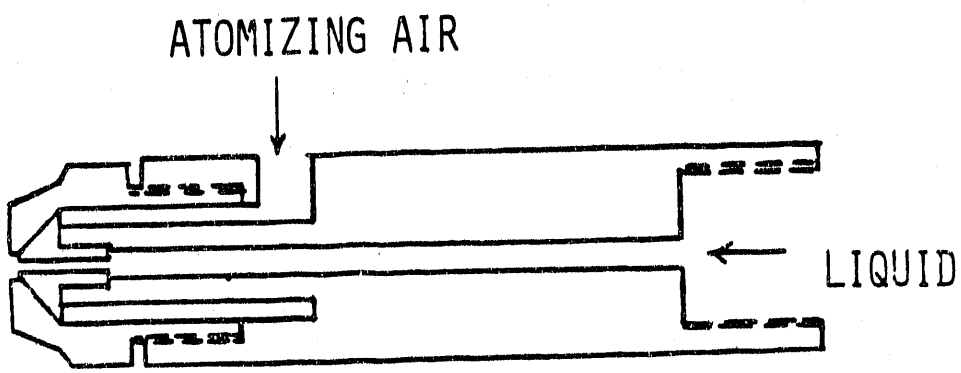

DISTRIBUTOR END VIEW

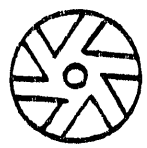

Fig. 2 Correlation between the flow behavior index of a concentrated suspension and the Hamaker constant (solid circles are data from Gadala-Maria and Acrivos, 1980 at volume fractions (ϕ 's) of 0.55, 0.45, and 0.40)

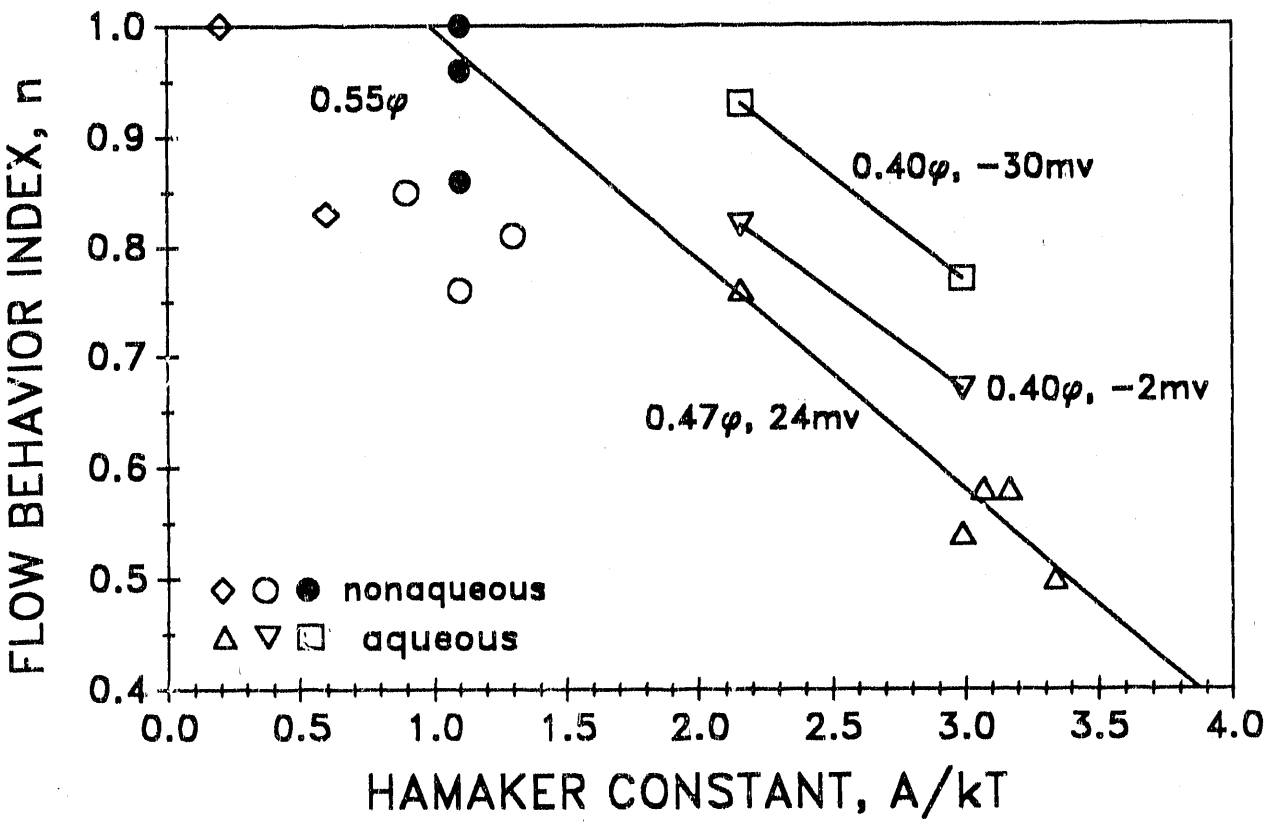

Fig. 3 The relative viscosity of a pseudoplastic suspension is independent of particle density

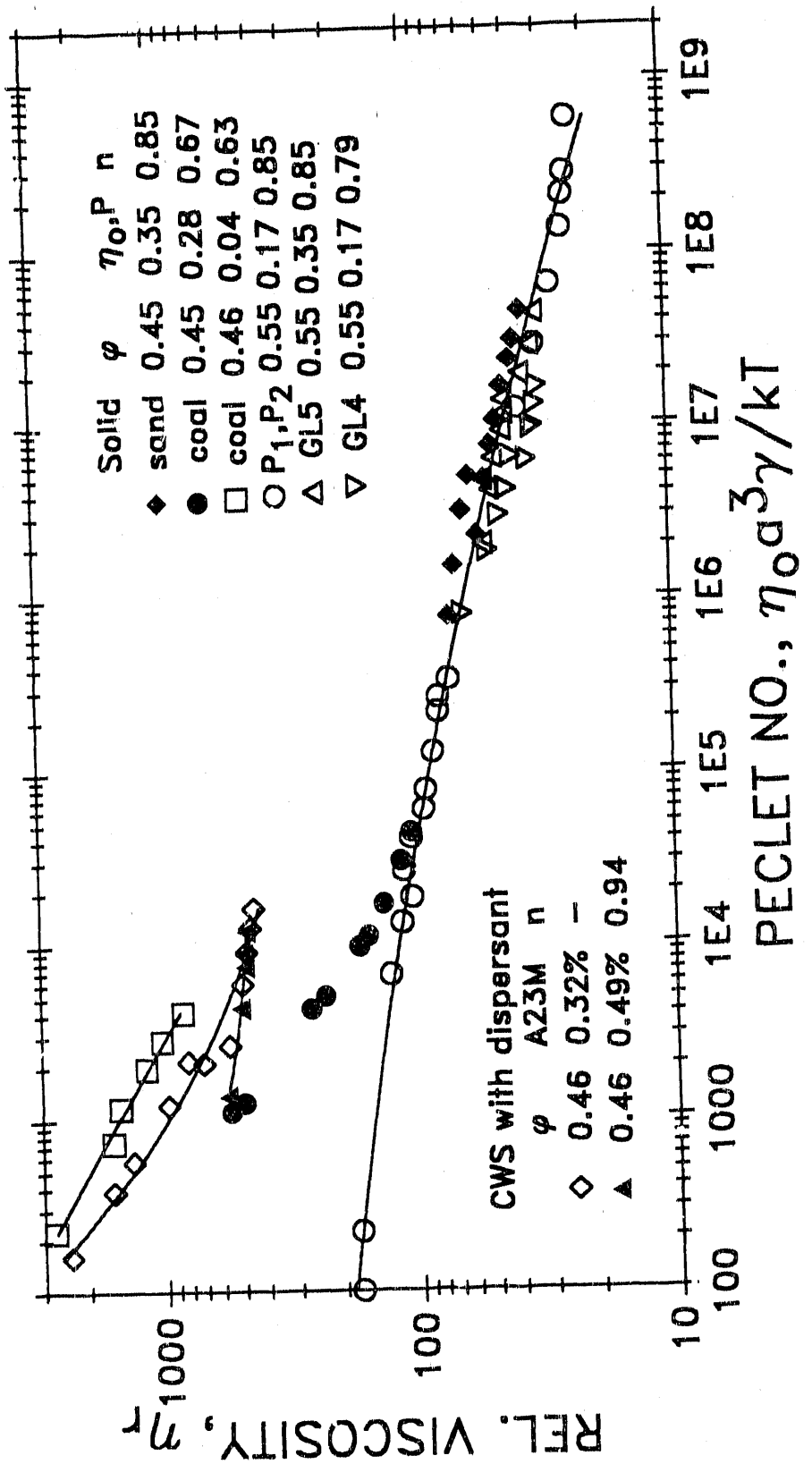

Fig. 4 Viscosity of micronized coal water slurry as a function of shear rate

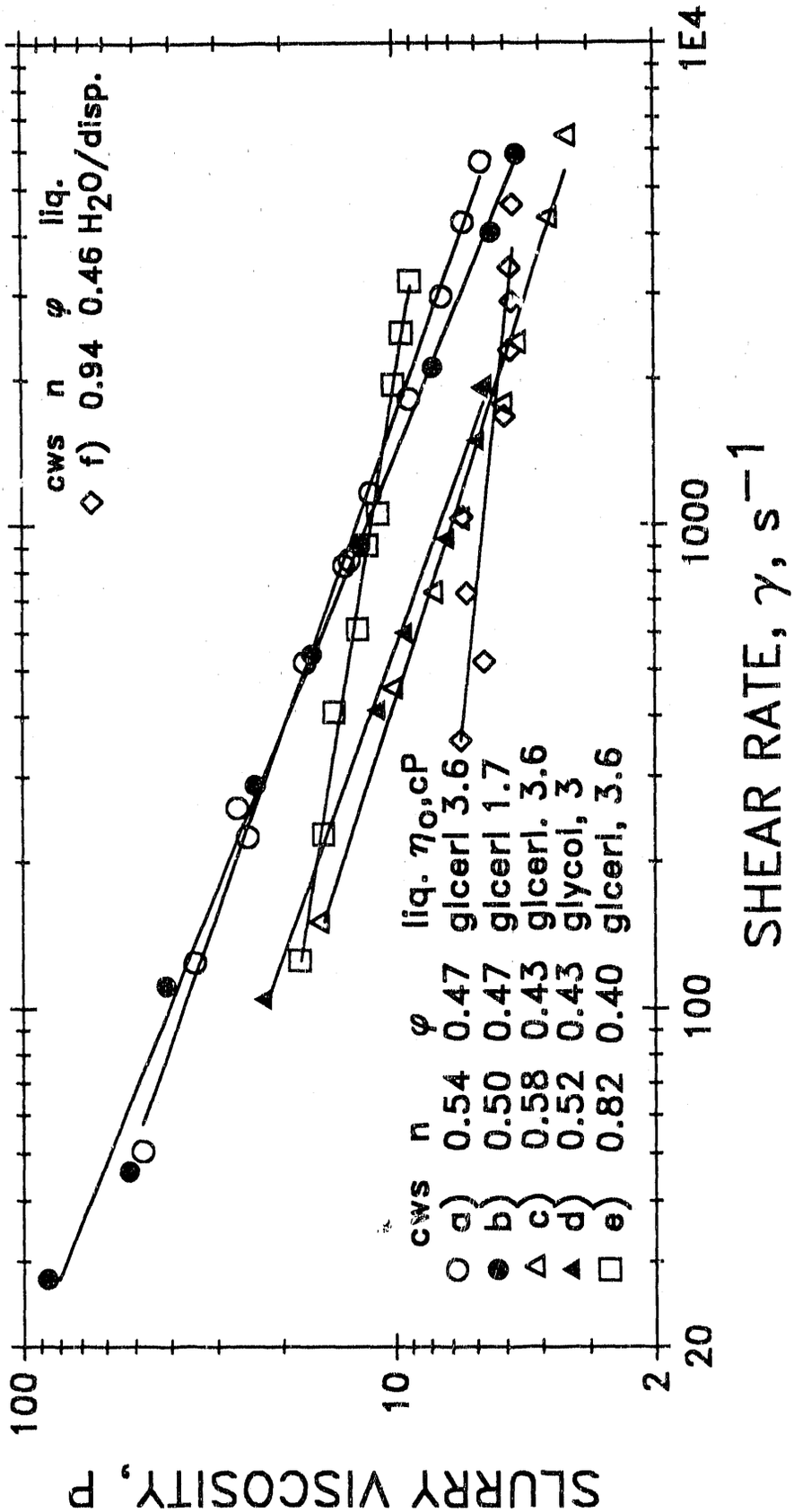

Fig. 5 Correlation between the wave mechanism based-models and the measured nondimensional drop MMDs at atomizing air pressures a) below and b) above the threshold pressure (multiply the nondimensional MMD from both axes by 15.2 to obtain the drop MMD in μm, diagonal lines represent perfect correlation)

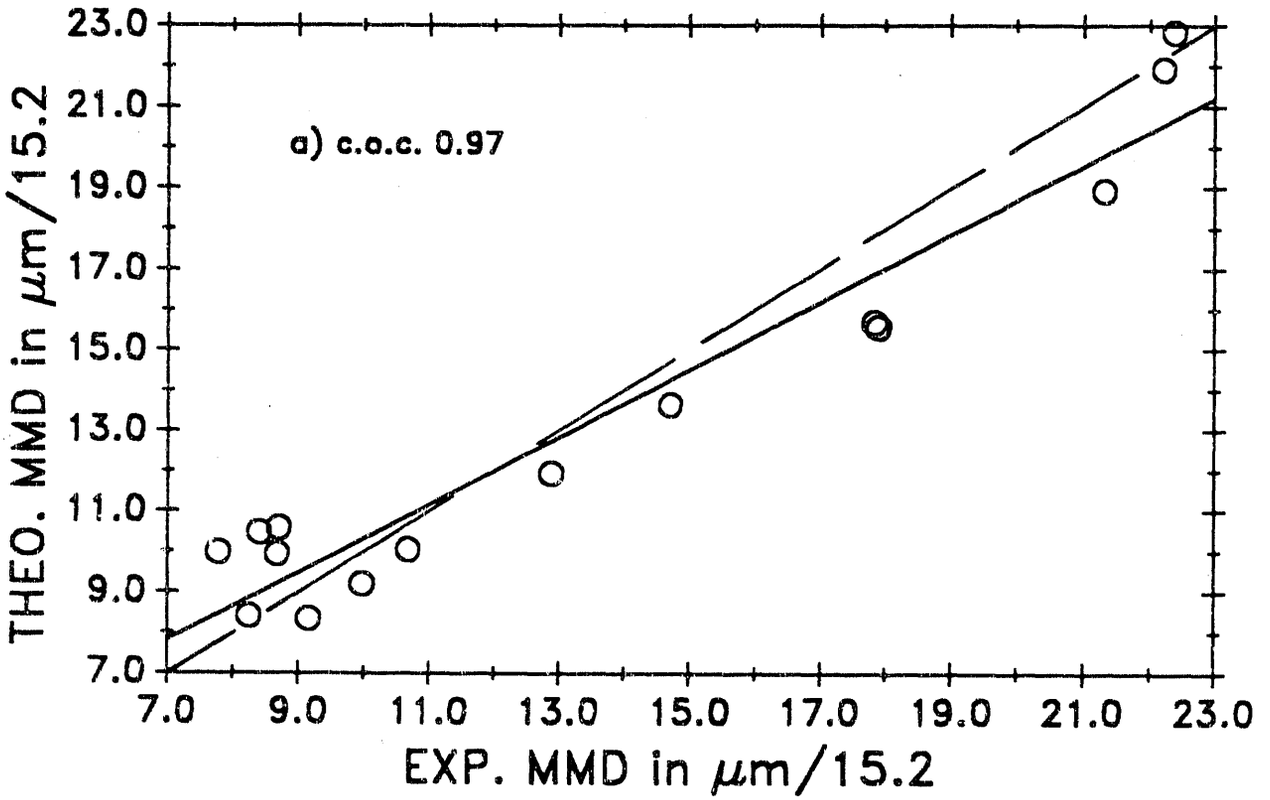

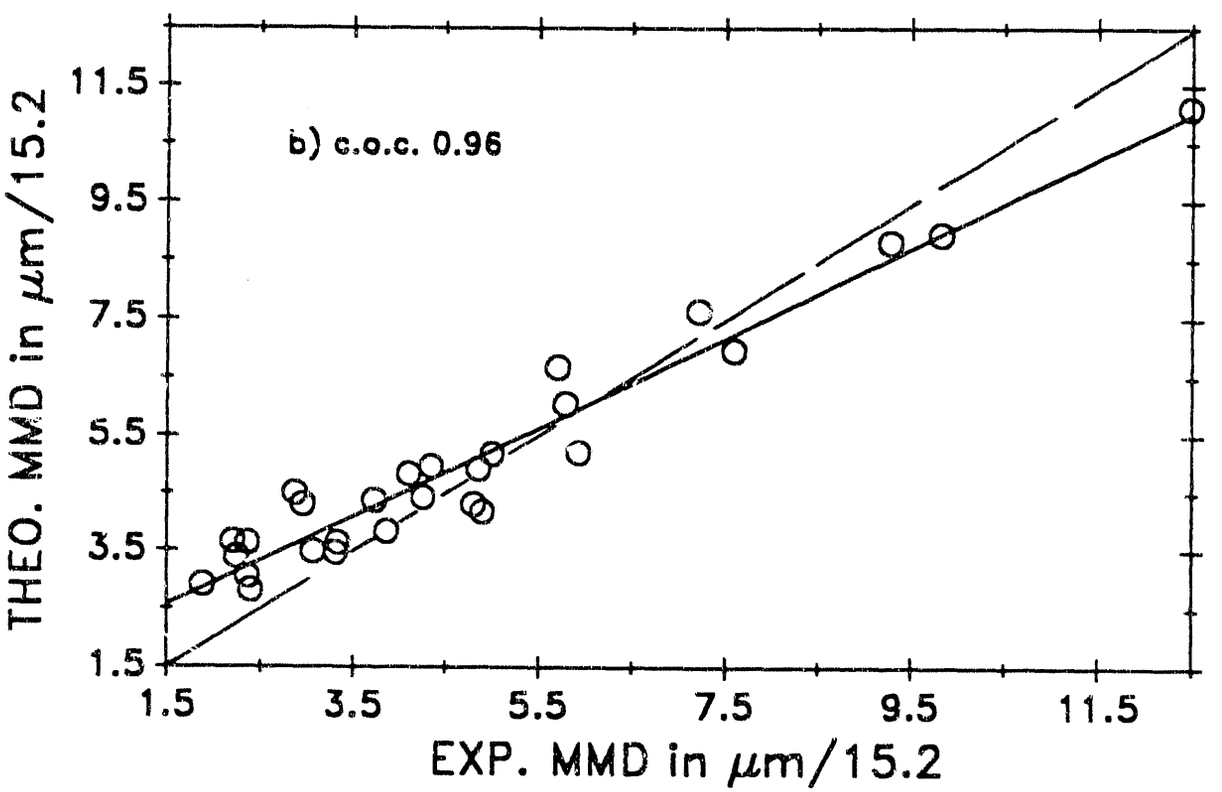

Fig. 6 Comparison of drop mass median diameters for atomized slurries (solid points) and atomized glycerol and its aqueous solution (open circles and open triangles), and atomized pseudoplastic polyethylene glycol (open diamonds)

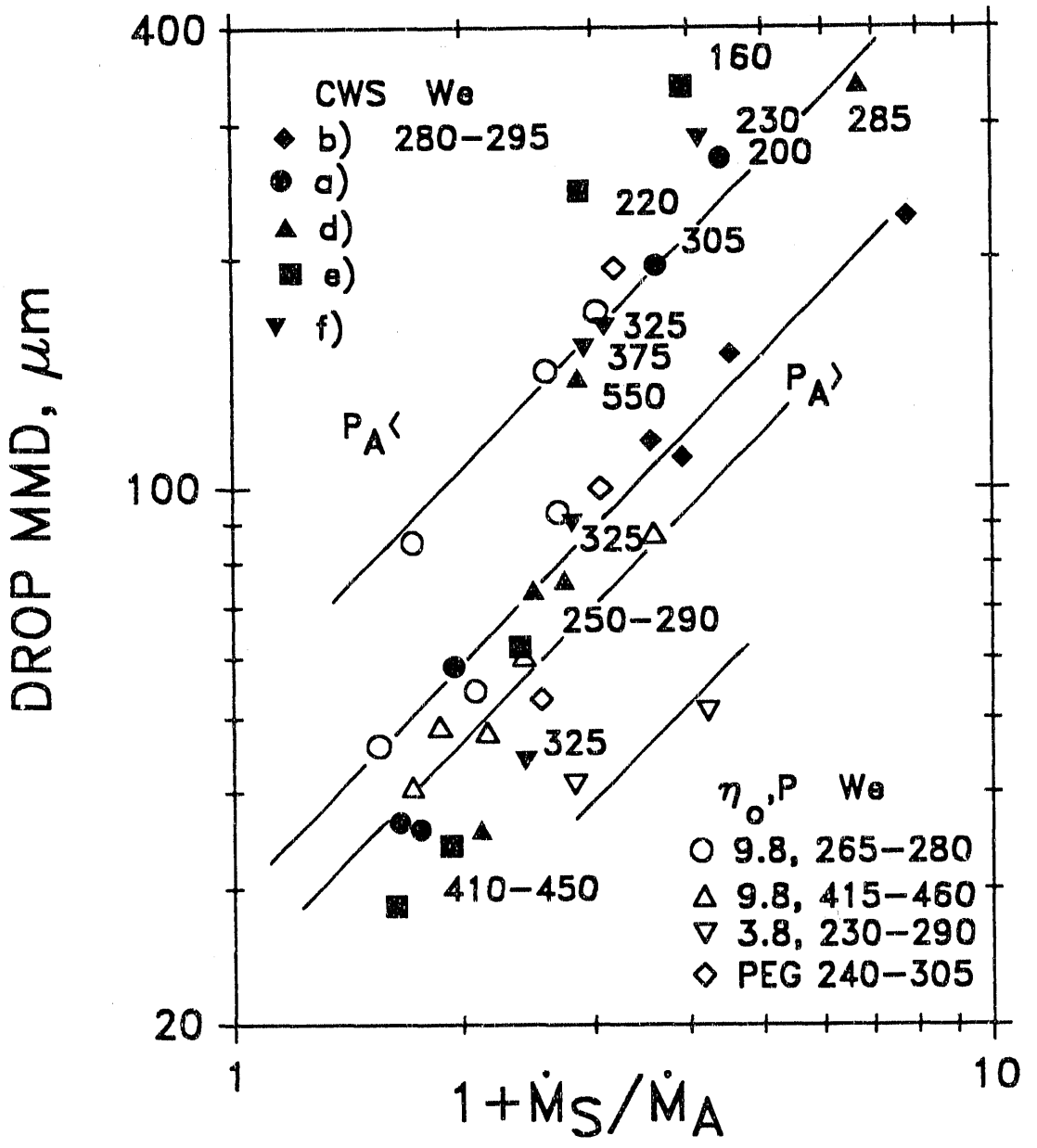

Fig. 7 Drop size distributions of slurries a) and c)

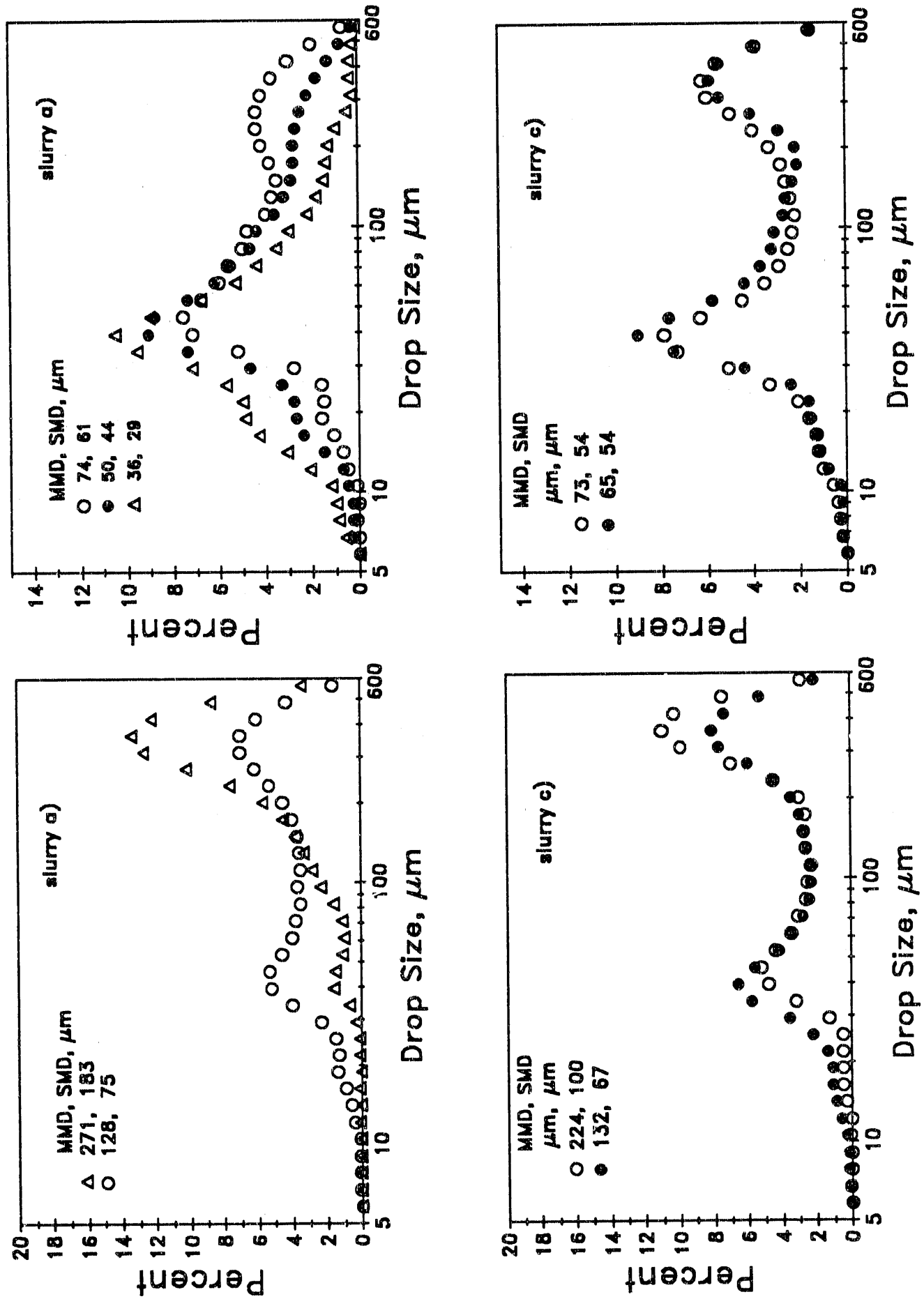

Fig. 8 Drop size distributions of slurries d) and f)

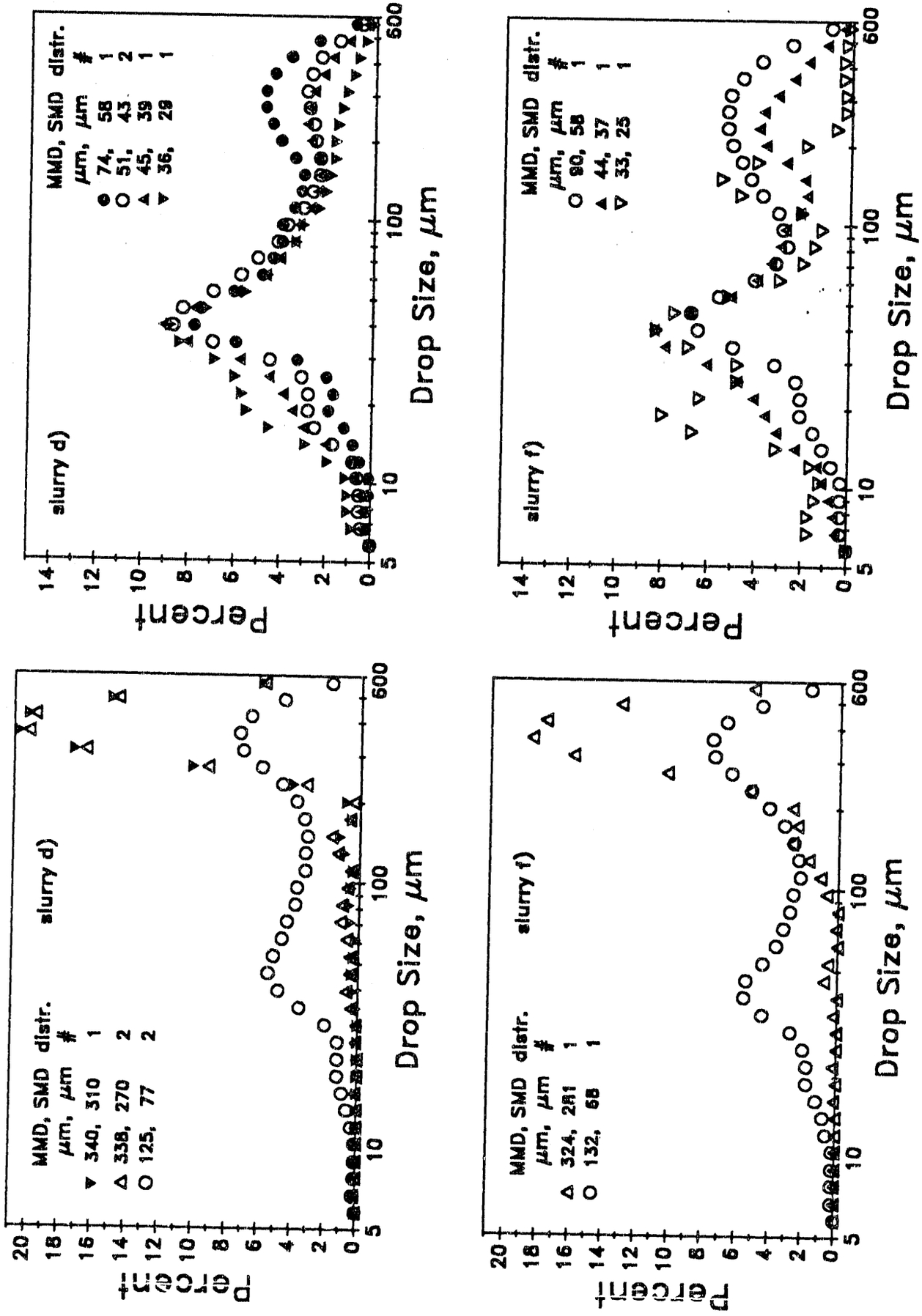

Fig. 9 Effects of distributor design on the mass flow rate of atomizing air as a function of inlet pressure

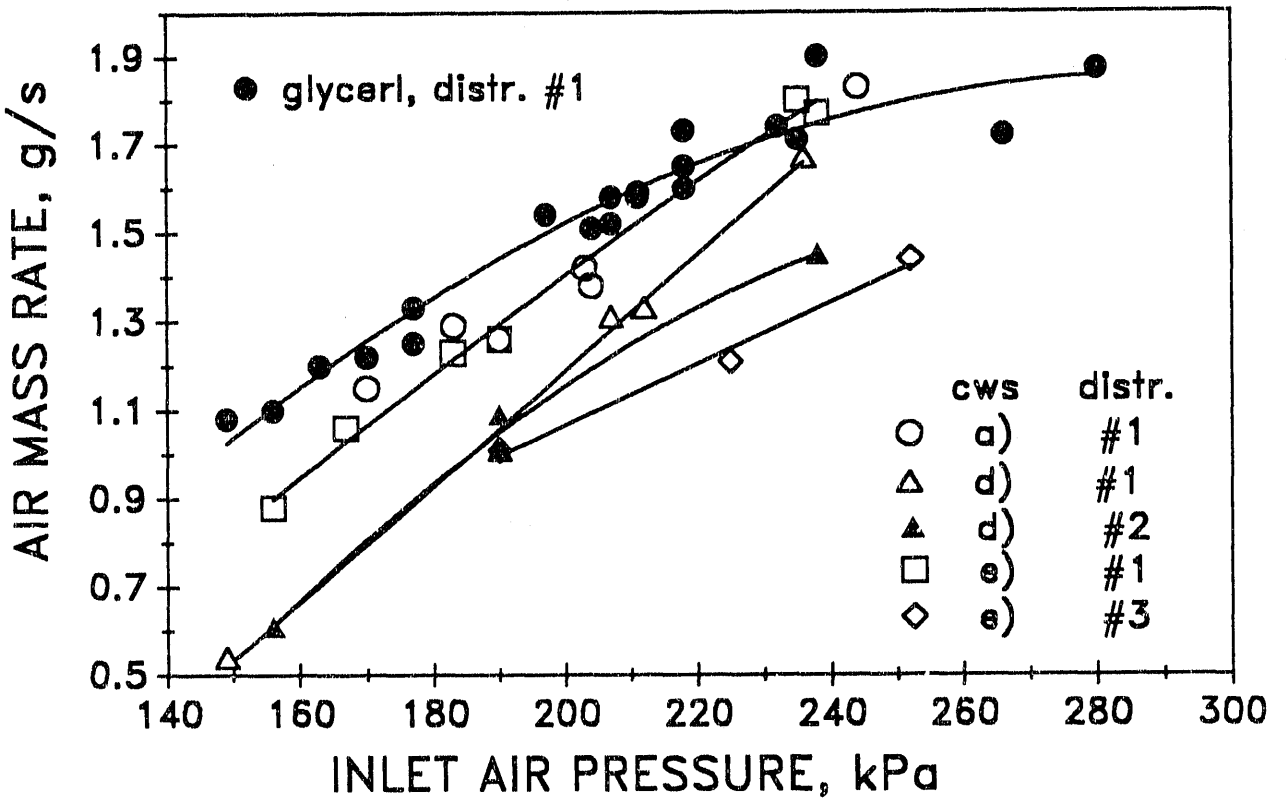

Fig. 10 Drop size distributions of glycerol (9.8 P), aqueous glycerol containing 92% glycerol (3.8 P), and polyethylene glycol mixture of 8000 and 600 molecular weights

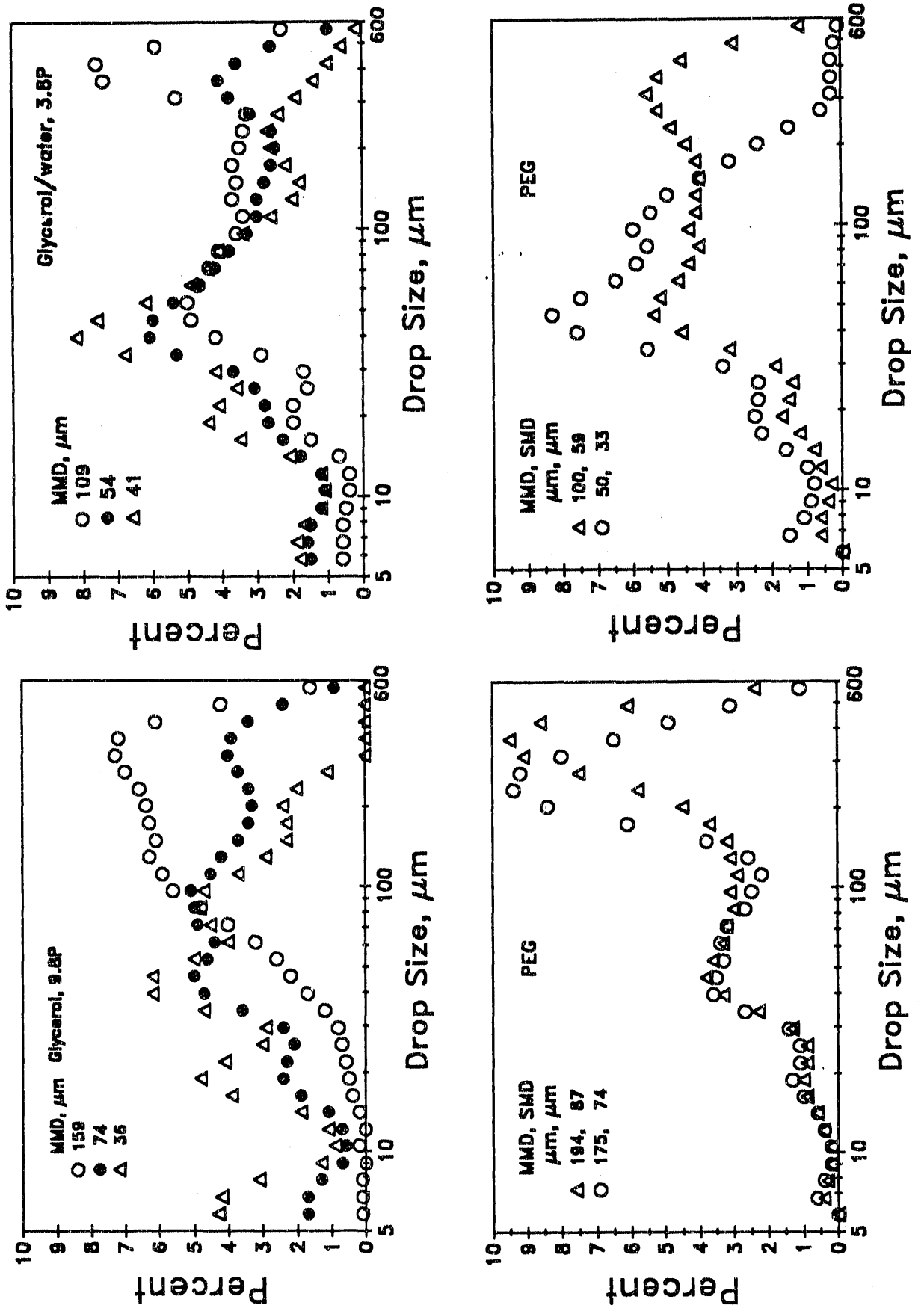

END

DATE FILMED

02 / 14 / 91